# The "Exceptionally Fresh" Udachnaya-East Kimberlite: Evidence for Brine and Evaporite Contamination

S. I. Kostrovitsky, M. G. Kopylova, K. N. Egorov, and D. A. Yakovlev

**Abstract**

The composition of the serpentine-free Udachnaya-East kimberlite containing alkali carbonate, gypsum, halite, and other Na-, Cl-, and S-rich minerals has been the basis for a model of alkali-rich primary kimberlite melt. The interpretation of these minerals as mantle-derived, however, contradicts geology and hydrogeology of the Yakutian kimberlite province, as well as petrographic, geochemical, and isotopic evidence. The Udachnaya-East pipe is similar to many other southern Yakutian kimberlites, which emplace through 2-km-thick evaporite-bearing terrigenous carbonate sediments saturated with brines. A secondary origin of Na-, Cl-, and S-rich minerals in the southern Yakutian kimberlites is supported by (1) a regional correlation between the geology and hydrogeology of the local country rocks and the kimberlite mineralogy, in particular the difference between southern and northern Yakutian kimberlites; (2) a restriction of halite or gypsum mineralization to certain depth horizons where pipes intersect country rock strata with similar mineralogy; (3) the localization of the highest abundances of Na–Cl–S-bearing minerals at a depth interval that correlates across three magmatic phases of kimberlites and coincides with the roof of the aquifer carrying Na brines; (4) the presence of evaporite xenoliths and veins of halite, gypsum, and carbonate cutting through kimberlite and xenoliths; (5) crystallization of halite and alkali carbonate after serpentine and other groundmass minerals as evidenced by the rock textures; (6) geochemical evidence for crustal contamination, including high bulk $CO_2$ and CaO content, the absence of correlation between bulk $Na_2O$ and any geochemical parameters, as well as initial Sr ratios, $\delta^{13}C$, $\delta^{18}O$, $\delta^{37}Cl$, and $\delta^{34}S$ intermediate between crustal and mantle values. We propose that the Udachnaya-East kimberlites acquired high Na, S, and Cl contents by interaction with buried Cambrian Na–Ca–Cl brines or assimilating evaporite xenoliths from the 500-m-thick Chukuck suite formed in the Daldyn-Markha carbonate bank.

Revised for the 10th IKC Proceedings Volume, November 2012.

S. I. Kostrovitsky (✉) · D. A. Yakovlev
Institute of Geochemistry SB RAS, Irkutsk, Russian Federation
e-mail: serkost@igc.irk.ru

M. G. Kopylova
Department of Earth & Ocean Sciences, University of British Columbia, Vancouver, Canada

K. N. Egorov
Institute of the Earth's Crust SB RAS, Irkutsk, Russian Federation

D. G. Pearson et al. (eds.), *Proceedings of 10th International Kimberlite Conference*, Volume 1, Special Issue of the Journal of the Geological Society of India,
DOI: 10.1007/978-81-322-1170-9_6, 

**Keywords**
Yakutian province • Udachnaya-East kimberlite pipe • Halite • Mantle • Brine • Evaporite xenolith • Primary kimberlite melt

## Introduction

Kimberlites are difficult rocks to study as they have a hybrid nature and combine several unequilibrated mineral parageneses. Kimberlite research is further complicated by late deuteric and secondary hydrothermal alteration. This alteration may lead to intense serpentinization of primary kimberlitic olivine. In Yakutian kimberlites, all olivine, microphenocrystal, macrocrystal, and megacrystal, is completely serpentinized, to the extent that the kimberlites are composed of 80–90 % serpentine and carbonates (e.g., Khar'kiv et al. 1991). In contrast to this, some kimberlites of the Udachnaya-East pipe show fresh, unserpentinized olivine and a lack of interstitial, late magmatic serpentine in the groundmass. The absence of all kinds of serpentine in the Udachnaya-East pipe gave rise to a theory that these kimberlites are "exceptionally fresh" in the global context (e.g., Kamenetsky et al. 2004; Maas et al. 2005). The composition of serpentine-free Udachnaya-East (SFUE) kimberlite was proposed as the best approximation of the deep kimberlite melt, which, unlike melt in other kimberlites, was not altered by late addition of crustal water. The authors further claimed that all serpentine in kimberlites is secondary and all hypabyssal kimberlites with interstitial groundmass serpentine, that is, all hypabyssal kimberlites in the world except the Udachnaya-East, are altered. As the composition of the SFUE kimberlite is poor in $H_2O$ and rich in Cl, K, and Na, these characteristics were assigned to the composition of the primary kimberlite melt equilibrated with the mantle (e.g., Maas et al. 2005; Kamenetsky et al. 2007a). This model provided an attractive explanation for compositions of fluid inclusions in fibrous diamonds, which are also rich in halogens and alkalis (e.g., Klein-BenDavid et al. 2009). The new model of the alkali-rich kimberlite melt has provided a new standard for mantle chlorine isotopes (Sharp et al. 2007) and has been used to constrain physical properties of the primary kimberlite melt (Kamenetsky et al. 2007a) and in numerous experimental studies of mantle melting.

To test this model, we collected geological data on the Udachnaya kimberlite and its country rocks. This geological background provides the basis for a petrographic and geochemical characterization of the SFUE kimberlite. The data suggest that the high Na, S, and Cl contents are the result of interaction with buried Cambrian Na–Ca–Cl brines or assimilation of evaporite xenoliths.

## Samples and Methods

SFUE kimberlite was sampled (34 specimens) in drill cores (holes 218 and 222) and in the open pit mine in 2000–2010 with a goal of building a representative collection of all kimberlite phases, including petrographic and mineralogical variations within the phases. As it is not possible to visually estimate a mode of Na-, S-, and Cl-rich minerals in the kimberlite, the selected specimens are not restricted to the extreme modes of these minerals.

Concentrations of ten major elements were analyzed by X-ray fluorescence (XRF) spectrometry on the SRM-25 Orelnauchpribor machine in the Geochemistry Institute Sib RAN (Irkutsk, Russia). The loss on ignition was determined at 950 °C in an induction furnace. Samples were then homogenized into fused beads from a 1:2 mixture of sample to lithium tetraborate at 1,100 °C in carbon glass containers in the induction furnace. The analysis was performed at 30 kV and current of 40 mA using an Rh anode X-ray tube. The standards were natural samples of carbonatite CI-2, basalt B-1, and peridotite P-1. The amount of FeO and $CO_2$ was determined for 0.2–0.3 g samples using HF–$HNO_3$–$HClO_4$ acid digestion and ammonium metavanadate titration. Chlorine was analyzed by XRF on S4 Pioneer spectrometer (AXS, Bruker), with a minimum detection limit of 0.01 % and a relative error <1 %. Water was determined gravimetrically using the Brush-Penfield method.

Trace elements were analyzed on an Elan 6100 DRC inductively coupled plasma mass spectrometer (Geochemistry Institute Sib RAN, Irkutsk, Russia) using HF–$HNO_3$–$HClO_4$ acid digestion. The precision of repeat trace metal measurements on standards was below 5 rel. % for Sr, La, Ce, Nd, Sm, Tb, Ho, Er, and Yb and 5–15 rel. % for Y, Zr, Pr, Eu, Gd, Dy, Tm, Lu, and Hf. Minimum detection limits for this analysis varied from 0.01 to 0.03 ppm.

The isotopic analysis of Sr was performed at the Geochemistry Institute Sib RAN (Irkutsk, Russia) with a Finnigan MAT-262 mass spectrometer. The analysis was carried out on the single band activation regime using $Ta_2O_5$ and the Re band. The measurements were normalized for the NBS

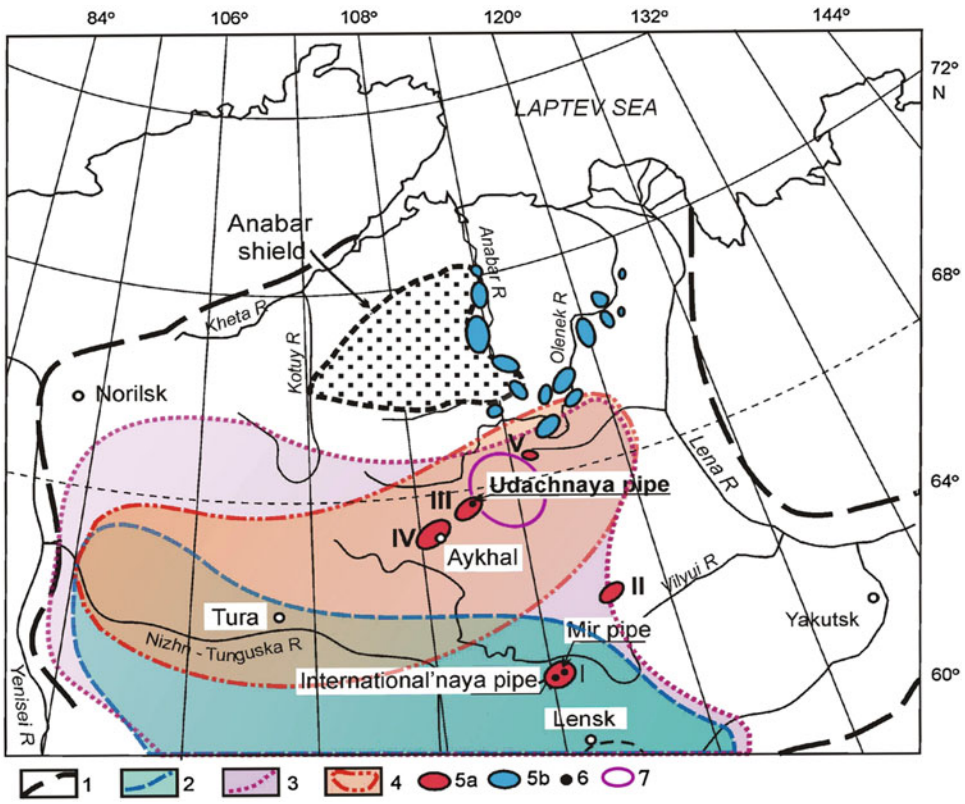


**Fig. 1** Kimberlite fields of the Siberian platform (Khar'kiv et al. 1998) with occurrences of salt-bearing deposits and brines (after Alekseev et al. 2007). *1–3* Boundaries of Siberian platform (*1*), the lower Cambrian evaporite-bearing sedimentary rocks (*2*), and brine occurrences (*3*); *4* zone of complete saturation of sedimentary cover in metamorphosed brine; *5* kimberlite fields: **a** southern diamondiferous (*I* Malobotuobiya, *II* Nakyn, *III* Daldyn, *IV* Alakit-Markha, *V* Verhnemuna) and **b** northern; *6* pipes; *7* Daldyn-Markha carbonate bank (Sukhov 2001; Polozov et al. 2008a, b; Drozdov et al. 2008)

SRM 987 standard. The value of $^{87}Sr/^{86}Sr$ during the analysis was determined as 0.710254 ± 11 ($n = 28$), with the relative error of 0.002 %.

## Geology of the Udachnaya Kimberlite

The Udachnaya kimberlite is emplaced into the Siberian craton and is part of the Yakutian kimberlite province. It is comprised of 20 fields (Fig. 1). Some of the 5 southern fields contain economic pipes, whereas the 15 northern fields are non-economic. The kimberlites erupted through Paleozoic terrigenous carbonate sediments, with a thickness of 1–3 km in the southern part of the kimberlite province and 0–1 km in the northern part (Brakhfogel 1984). The sediments are Cambrian and Ordovician limestone, dolomite with minor marls, evaporites, mudstone, and sandstone (Bobrievich et al. 1959).

The 353–367 Ma Udachnaya pipe from the Daldyn field was emplaced through the Lower to Upper Cambrian sedimentary rocks (limestones, dolomites, argillites, sandstones, and conglomerates) over 2 km thick (Fig. 2). The 400-m-thick Upper Cambrian clays and carbonates are underlain by clastic dolomite of the Chukuck suite at depths of 420–900 m. It, in turn, lies above the Early Cambrian limestones and sandstones. Although the kimberlite does not intersect massive evaporites, the clastic dolomite of the Chukuck suite contains halite and gypsum cement, and the total mode of halite in some Chukuck dolomites may reach 20–30 %. For example, the drill core 2 km to the northeast of the pipe cuts through halite-rich dolomite layers 1–3 m thick. The dolomite contains numerous karst cavities infilled with halite, gypsum, oil, and bitumen. The Chukuck suite in proximity to Udachnaya varies in thickness from 20–50 to 400 m based on drilling. The Chukuck suite and the coeval 520 Ma sedimentary rocks are thought to have accumulated in the sabkha environment (Polozov et al. 2008a, b) in a supratidal arid coastline and lagoon setting on a shallow bank with reefs (Fig. 3). This Daldyn-Markha carbonate bank (Sukhov 2001; Drozdov et al. 2008) is mapped in the area 200 by 50 km, encompassing the Udachnaya pipe (Fig. 1).

## Hydrogeology of the Udachnaya Kimberlite

The southern kimberlite fields of the Yakutian province that host economic diamond deposits occur in platform areas where thick sediments contain buried ancient groundwater (Fig. 1) that varies in composition from ultrafresh to Na–Ca brines. Brines are sealed in continuous, 1,200-m-thick unit of gypsum-bearing Cambrian limestones, dolomites, and halite (Alekseev et al. 2007). Two of the southern kimberlite fields—Daldyn and Alakit-Markha (III, IV on Fig. 1)

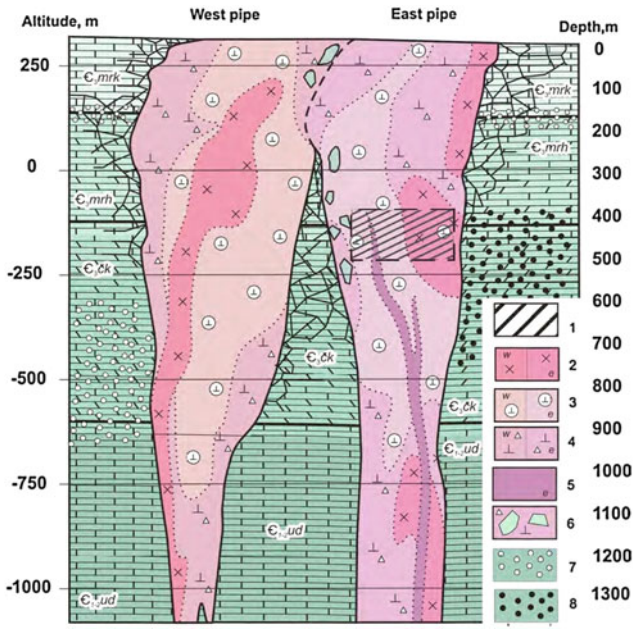


**Fig. 2** A geological cross section of the Udachnaya kimberlite. *1* SFUE kimberlite; *2* phase 1 of hypabyssal kimberlites; *3* phase 2 of volcaniclastic kimberlite breccia; *4* phase 3 of massive volcaniclastic kimberlite breccia; *5* phase 4 of hypabyssal dyke kimberlites; *6* large blocks of country rocks in kimberlite; *7* Ca–Cl waters in the *upper* and *lower aquifers*; *8* Na–Cl waters in the *lower aquifer*. *Country rocks* $Є_{1-2}$ud (the Udachnaya suite, 500–600 m)—limestones, carbonate sandstones, gravelites, $Є_3$ck—the Chukuck suite, 260–340 m, coarse clastic dolomites and limestones cemented by cryptocrystalline calcite and gypsum. The middle part of the suite comprises karst dolomite with leached cavities infilled with gypsum, halite, bitumen, and oil. $Є_3$mrh (the Markha suite, 370 m thick)—limestones and dolomites with occasional beds of carbonate siltstone and argillite. $Є_{13}$mrk (the Morkoka suite, 220 m thick)—interstratified dolomitized limestones, dolomites, carbonate siltstones, argillites, carbonate conglomerates, and sandstones

(containing Udachnaya and Aykhal pipes, among others)—are situated within the zone of complete saturation of the sedimentary cover in metamorphosed highly mineralized brines (>0.2–0.4 g/cm$^3$) (Alekseev et al. 2007). In contrast to the southern kimberlite fields, the northern kimberlites erupt through buried low mineralized waters (0.03–0.05 g/cm$^3$) (Khar'kiv et al. 1991).

The Udachnaya kimberlite cuts through 2 aquifers (Drozdov et al. 1989 and Fig. 2) of the Olenek artesian basin. The upper aquifer was restricted to the fractured kimberlite close to the eroding surface and had disappeared after mining deepened the open pit. The roof of this aquifer was situated at 150–220 m into the mine pit. The thickness of the aquifer was no more than 5–10 m. The waters ($Mg_{40}Ca_{44}Na_{14}K_2$ $Cl_{98.2}Br_{0.7}$ $SO_{41.0}$ $HCO_{3\ 0.1}$) were Cl and Ca brines, with traces of Br, B, Rb, Li, and Sr and mineralization equal to 91.4 g/dm$^3$ (Drozdov et al. 2008). The lower aquifer of the Olenek artesian basin is mapped below 350 m to the east of the pipe and below 630 m to the west of the pipe. The aquifer has a very pronounced arched relief of the roof; the highest point of this convex roof is 200–250 m higher than that of the aquifer roof in the Udachnaya West and in the sedimentary country rocks (Fig. 4). This arched aquifer is hosted by clastic dolomites of the Chukuck suite and porous, sponge-like kimberlites with high permeability, comparable to that of the dolomites. Hydrogeological studies confirm that the clastic dolomites have a hydraulic connection with the porous kimberlites (Drosdov et al. 1989, 2008). The aquifer changes its hydrological properties and the composition of the water from the east to the west of the pipe. The latter has a low internal pressure and flow rate, similar to the sedimentary country rocks. The waters are Ca–Cl brines with composition $Mg_{19,5}Ca_{56.8}Na_{18.6}K_{5.1}$ $Cl_{99}Br_{0.85}$ $SO_{4\ 0.05}HCO_{3\ 0,0.1}$ and mineralization equal to 300–380 g/dm$^3$ (Drozdov et al. 2008). The aquifer of the Udachnaya-East kimberlite has a high hydraulic pressure. The waters are Na–Cl brines with composition $Mg_{4.4}Ca_{5.4}Na_{82.2}K_8$ $Cl_{99.1}Br_{0.47}$ $SO_{4\ 0.42}HCO_{3\ 0.01}$ and mineralization of 322 g/dm$^3$ (Drozdov et al. 2008). These anomalously sodic brines are restricted to the Chukuck suite of the Daldyn-Markha bank. The waters of the lower aquifer flow into the underground Udachnaya mine and deposit abundant halite and gypsum in the Udachnaya open pit (Fig. 4).

## Geology and Mineralogy of the Udachnaya-East Kimberlite

The Udachnaya kimberlite comprises two separate pipes, the older West and the younger East pipe, that merge at 250 m below the present surface. Each of the Udachnaya pipes formed through 3–5 eruptive phases (Khar'kiv et al. 1991; Zinchuk et al. 1993) (Fig. 2). The East pipe is infilled with early hypabyssal kimberlite, commonly occurring on pipe margins (Fig. 2) and several phases of volcaniclastic kimberlite breccia cut by 10–50-cm-thick dykes of hypabyssal monticellite kimberlite (Kornilova et al. 1998). The breccia commonly contains clasts of early olivine- and calcite-rich hypabyssal kimberlite and occasionally clasts of olivine-, diopside-, and phlogopite-rich hypabyssal kimberlite (Egorov et al. 1986). The Udachnaya West kimberlite hosts serpentinized olivine through the entire explored depth (1,200 m), whereas the profile of olivine serpentinization of the Udachnaya-East kimberlite is complex. In the upper 400 m of the kimberlite, olivine is 80–95 % serpentinized; at 400–500 m, it is fresh; and at 700–1,200 m, the degree of serpentinization gradually increases to 100 %.

The SFUE kimberlite at 400–500 m depth (Fig. 2) was first described in 1976 (Marshintsev et al. 1976). The serpentine-free kimberlite comprises all 3 magmatic phases of the pipe at this depth. The contact between SFUE kimberlite

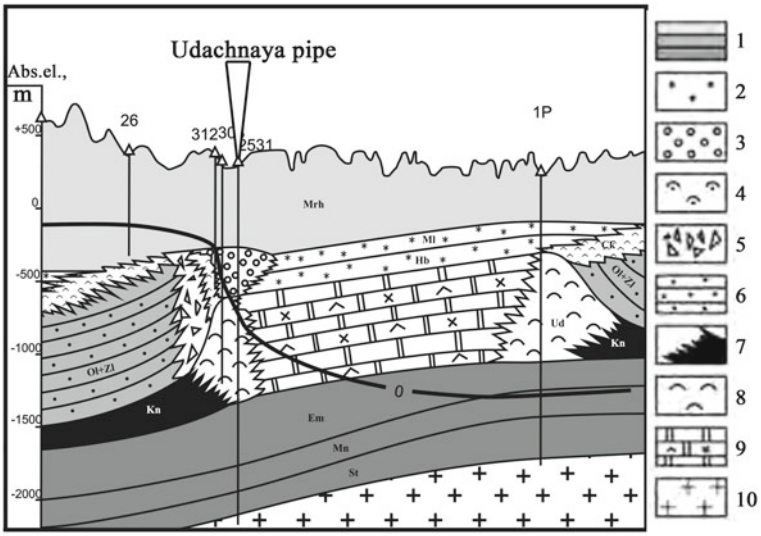


**Fig. 3** A cross section through the Daldyn-Markha carbonate bank (Polozov et al. 2008a, b; Sukhov 2001; Kononov 2009) showing localization of the Udachnaya pipe. *1* Cambrian carbonates, *2* sabha deposits, *3* carbonate bar deposits, *4* terrigenous carbonate rock marls and dolomite breccias, *5* carbonate terrigenous rocks, *7* black shales, *8* reef rocks, *9* lagoon sulfate–salt–carbonate rocks, *10* granite–gneiss basement


**Fig. 4** **a**, **b** Deposition of modern halite in the Udachnaya open pit at the 450–480 m level in 2008; **c**, **d** geodes in a leached kimberlite partly (**c**) or completely (**d**) infilled with gypsum

and more common kimberlites with serpentinized olivine is very sharp even on the scale of a single thin section (Fig. 5). The SFUE kimberlite is predominantly fragmental, containing 1–30 % xenoliths of country rocks and clasts of early massive hypabyssal phlogopite kimberlite (Egorov et al. 1986). The matrix of the SFUE kimberlite breccia is composed of phenocrystal olivine and calcite, with varied abundances of interstitial shortite, zemkorite, halite, sylvine, phlogopite, apatite, perovskite, and Ti-magnetite (Egorov et al. 1986; Kamenetsky et al. 2004, 2007a). The groundmass of hypabyssal diopside–phlogopite kimberlite found as clasts is composed of euhedral olivine microphenocrysts (20–25 %), phlogopite (30–35 %), and clinopyroxene (15 %) set in a fine-grained aggregate of carbonate, sodalite, shortite, opaque minerals, and interstitial shortite (Egorov et al. 1986). Textural relationships of S-, Na-, and Cl-rich minerals in thin sections demonstrate their crystallization in sequence serpentine − anhydrite + carbonate − halite (Pavlov and Ilupin 1973). Similar conclusions on the late crystallization of halite, shortite, and zemkorite with respect to other matrix and groundmass minerals have been made by Kornilova et al. (1998) and Egorov et al. (1988). The SFUE kimberlite breccia is cut by dykes of the SFUE coarse macrocrystal monticellite kimberlite (Kornilova et al. 1998). In contrast to the breccias, the groundmass of the late hypabyssal macrocrystal kimberlite contains up to 15–20 % monticellite and lower modes of carbonate minerals (Kornilova et al. 1998).

All varieties of SFUE kimberlite show development of secondary carbonate. Recrystallization of calcite makes it more coarse-grained and forms monomineralic calcite veins. SFUE kimberlite is also cut by late fine-grained gypsum veinlets and coarse veins of gypsum occasionally reaching 20 m in thickness. The kimberlite often hosts geodes with carbonate–chloride–gypsum minerals precipitated in late leached cavities (Fig. 4c–d). The SFUE kimberlite carries large angular xenoliths of carbonate–halide composition with thermally metamorphosed blue selvages (Fig. 6).

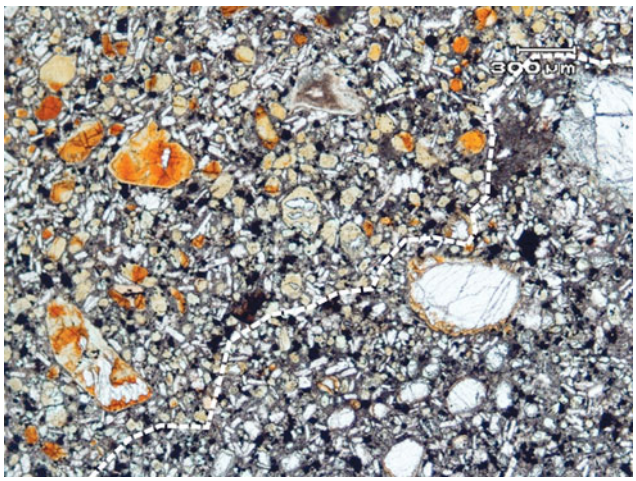


**Fig. 5** A photomicrograph of hypabyssal SFUE kimberlite with calcite microlites. Note the sharp boundary between kimberlite with serpentinized olivine (SFUE, *upper left corner*) and kimberlite with fresh olivine (*low right corner*)

## Bulk Composition

Major and trace element compositions of the SFUE kimberlite are reported in Tables 1, 2, and 3. The compositions were determined for 3 kimberlite phases: (1) the early hypabyssal kimberlite that occurs as clasts in breccia; (2) the kimberlite breccia; and (3) the coarse macrocrystal monticellite kimberlite occurring in late dykes. Oxide contents averaged by the kimberlite phase (Table 1) show

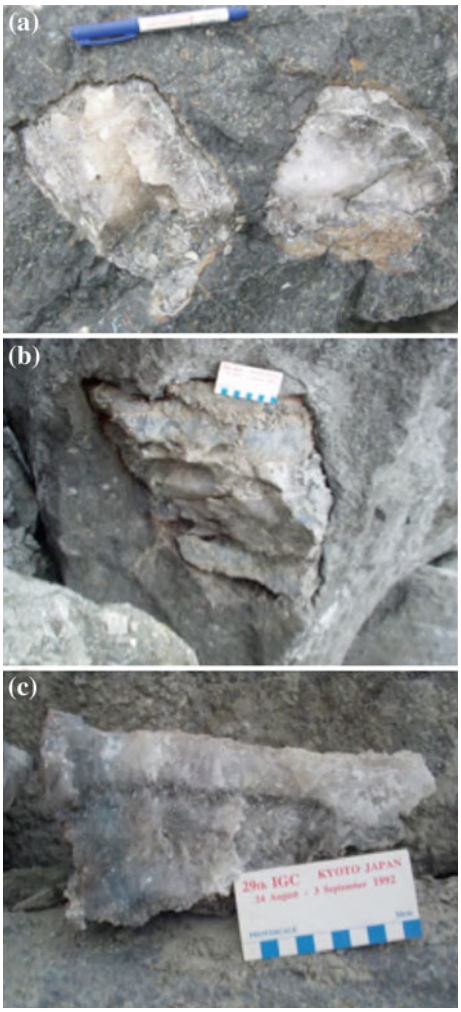


**Fig. 6** Xenoliths of halite in the Udachnaya-East kimberlite. Note angular shapes of the xenoliths and a blue thermally metamorphosed margin of the xenolith on photograph C (Polozov et al. 2008a, b)

**Table 1** Statistical parameters for major element compositions (in wt.%) for SFUE kimberlites of different phases

| Number of analyses | Phase 1 hypabyssal kimberlite | Kimberlite breccia | Dyke hypabyssal kimberlite |
|---|---|---|---|
| | 19 | 11 | 3 |
| $SiO_2$, wt.% | **29.0 ± 2.4** | **28.2 ± 2.19** | **26.8 ± 4.2** |
| | *24.1 – 33.3* | *24.7 – 31.5* | *23.5 – 31.5* |
| $TiO_2$ | **1.64 ± 0.48** | **1.37 ± 0.38** | **1.8 ± 0.51** |
| | *0.96 – 2.91* | *0.53 – 1.83* | *1.5 – 2.38* |
| $Al_2O_3$ | **2.22 ± 0.5** | **2.13 ± 0.46** | **2.2 ± 0.43** |
| | *1.51 – 3.21* | *1.66 – 3.3* | *1.85 – 2.68* |
| $Fe_2O_3$ | **3.3 ± 1.17** | **3.47 ± 0.52** | **4.6 ± 1.36** |
| | *0.84 – 5.66* | *2.56 – 4.05* | *3.14 – 5.86* |
| FeO | **5.84 ± 1.0** | **5.31 ± 1.08** | **5.8 ± 1.47** |
| | *4.08 – 7.9* | *3.33 – 7.25* | *4.77 – 7.5* |
| MnO | **0.16 ± 0.03** | **0.15 ± 0.03** | **0.19 ± 0.04** |
| | *0.12 – 0.21* | *0.08 – 0.19* | *0.16 – 0.23* |
| MgO | **31.4 ± 2.93** | **31.0 ± 2.38** | **30.5 ± 2.97** |
| | *24.9 – 36.4* | *26.7 – 35.5* | *27.7 – 33.6* |
| CaO | **13.3 ± 3.15** | **13.7 ± 2.44** | **14.2 ± 1.51** |
| | *7.47 – 19.1* | *9.25 – 16.8* | *12.4 – 15.14* |
| $Na_2O$ | **0.70 ± 0.85** | **0.79 ± 0.94** | **0.26 ± 0.06** |
| | *0.07 – 2.82* | *0.09 – 3.1* | *0.19 – 0.3* |
| $K_2O$ | **0.94 ± 0.35** | **1.29 ± 0.53** | **1.16 ± 0.27** |
| | *0.42 – 1.63* | *0.57 – 2.07* | *0.92 – 1.45* |
| $H_2O$ | **2.02 ± 1.36** | **1.98 ± 1.41** | **1.71 ± 1.09** |
| | *0.24 – 5.49* | *0.55 – 4.19* | *0.87 – 2.94* |
| $CO_2$ | **8.17 ± 3.27** | **9.58 ± 2.91** | **9.2 ± 3.25** |
| | *3.19 – 17.1* | *5.83 – 14.5* | *5.43 – 11.2* |
| $P_2O_5$ | **0.47 ± 0.12** | **0.48 ± 0.16** | **0.53 ± 0.15** |
| | *0.30 – 0.79* | *0.30 – 0.85* | *0.36 – 0.66* |
| F | **0.16 ± 0.06** | **0.16 ± 0.06** | **0.14 ± 0.05** |
| | *0.09 – 0.3* | *0.06 – 0.22* | *0.08 – 0.17* |
| Cl | **0.67 ± 0.44** | **0.73 ± 0.67** | |
| | *0.33 – 1.53* | *0.34 – 2.23* | *0.46 – 0.52* |

*Comment* The *bold values* in each cell refer to mean contents ± standard deviation of two sigma; the *numbers in italics* refer to the minimum and maximum values of oxide contents

that the early hypabyssal kimberlite and hypabyssal kimberlite of late dykes are richer in $FeO_{tot}$ and $TiO_2$ than the breccia. Phlogopite kimberlite (sample Eg-Phl in Table 2) is characterized by extremely high contents of $TiO_2$, $FeO_{tot}$, and $K_2O$ at very low concentrations of MgO and $CO_2$. The main trend in the major element composition for all 3 phases of the SFUE kimberlite shows an inverse correlation of CaO with $SiO_2$ and MgO, typical of all worldwide kimberlites.

The content of $Na_2O$ (0.07–3.1 wt.%, 0.74 wt.% on average) in the Udachnaya-East kimberlite is higher than that of a typical kimberlite (0.16 wt.% $Na_2O$ in Group I southern African kimberlite, Becker and Le Roex 2006). In our samples, sodium oxide is the only major element oxide that does not correlate with any other oxides, including $H_2O$.

An interesting pattern is observed in the covariation of $Na_2O$ and $CO_2$. There is a threshold concentration of 9 wt.% $CO_2$, above which $Na_2O$ content in kimberlite does not exceed 0.5 wt.%. Since much of $CO_2$ reside in secondary carbonate, this pattern could be interpreted as sealing of carbonated kimberlite to Na–Cl brines.

Concentrations of $Na_2O$ and Cl in the Udachnaya-East vary widely. In our analyzed samples, the chlorine content is 0.3–2.2 wt.%. Depth-dependent Cl and $Na_2O$ concentrations have been found by previous studies. The subsurface levels above 160 m in Udachnaya-East are characterized by low (<0.2 wt.%) $Na_2O$ and Cl contents, which increase below 160 m (Pavlov and Ilupin 1973). The highest contents of $Na_2O$ and Cl (up to 9 wt.%) are reached in SFUE kimberlites at 400–500 m (Kamenetsky et al. 2007a). Elevated Cl levels (2.2–4.2 wt.% Cl) are also noted at 760–860 m (Pavlov and Ilupin 1973). Superimposed on these depth patterns are spatially localized heterogeneities in the $Na_2O$ and Cl contents within a depth horizon. It is interesting that the kimberlites of the three magmatic phases locally demonstrate identical contents of $Na_2O$ and $H_2O$, although the contents vary widely depending on the sample location. This is shown for kimberlites of 3 phases (the hypabyssal kimberlite clasts in breccia, the breccia, and the late hypabyssal dykes) sampled in 6 locations in the 400–500-m depth interval (Fig. 7). The contents of $H_2O$, $Na_2O$, and, by inference, the mode of halite are thus controlled only by the spatial position of the kimberlite specimen, rather than by the composition of the kimberlite melt.

Trace element patterns of all 3 phases of the SFUE kimberlite demonstrate identical shapes at different absolute concentrations (Fig. 8, Table 3). The early hypabyssal kimberlite is richer in incompatible elements than in the breccia, while the highest concentrations of trace elements are found in the late hypabyssal kimberlite dykes.

## Strontium Isotope Composition of Halite in the Udachnaya Kimberlite

We analyzed $^{87}Sr/^{86}Sr_i$ ratios for different textural varieties of halite, including salts deposited by brines in the open pit (Fig. 4), angular xenoliths of halite (Fig. 6), and a coarse halite–sylvine geode in a secondary leached cavity in the kimberlite. Salts deposited in the Udachnaya-East open pit have a $^{87}Sr/^{86}Sr_i$ of 0.708348, whereas extreme $^{87}Sr/^{86}Sr_i$

**Table 2** Bulk compositions (in wt.%) of the Udachnaya-East SFUE kimberlite from mine level 400–500 m

| Sample number | 1 | 2 | 3 | 4 | 5 | 6 | 7 | 8 | 9 |
|---|---|---|---|---|---|---|---|---|---|
| | 07-6d | 07-6b | 01-213k | 01-213b | 05-75k | 05-75b | 00-137k | 00-137b | 10-4d |
| $SiO_2$, wt.% | 25.34 | 24.75 | 28.08 | 30.32 | 30.20 | 29.00 | 24.06 | 25.68 | 23.49 |
| $TiO_2$ | 1.50 | 1.06 | 2.48 | 1.83 | 1.45 | 1.83 | 1.09 | 0.53 | 2.38 |
| $Al_2O_3$ | 1.85 | 1.96 | 2.41 | 1.82 | 1.85 | 1.98 | 2.19 | 1.66 | 2.68 |
| $Fe_2O_3$ | 4.68 | 3.99 | 5.66 | 3.88 | 3.71 | 3.99 | 0.84 | 3.48 | 5.86 |
| FeO | 4.77 | 3.33 | 5.19 | 5.49 | 5.39 | 5.63 | 5.4 | 3.73 | 5.17 |
| MnO | 0.17 | 0.12 | 0.21 | 0.15 | 0.14 | 0.18 | 0.13 | 0.08 | 0.23 |
| MgO | 30.13 | 26.66 | 29.95 | 34.08 | 32.81 | 30.67 | 24.93 | 30.71 | 27.67 |
| CaO | 14.97 | 16.75 | 16.98 | 11.57 | 11.74 | 15.07 | 19.12 | 16.77 | 15.14 |
| $Na_2O$ | 0.19 | 0.24 | 0.49 | 0.66 | 1.21 | 1.25 | 0.08 | 0.16 | 0.30 |
| $K_2O$ | 1.11 | 2.03 | 0.42 | 1.03 | 0.55 | 0.57 | 0.70 | 1.47 | 1.45 |
| $H_2O$ | 1.32 | 1.61 | 0.24 | 0.55 | 2.49 | 1.30 | 3.43 | 3.86 | 2.94 |
| $CO_2$ | 10.97 | 14.54 | 6.25 | 7.49 | 7.08 | 6.79 | 17.1 | 13.15 | 11.16 |
| $P_2O_5$ | 0.56 | 0.30 | 0.79 | 0.36 | 0.37 | 0.64 | 0.30 | 0.85 | 0.66 |
| F | 0.17 | 0.20 | 0.15 | 0.20 | 0.09 | 0.09 | 0.15 | 0.11 | 0.16 |
| Cl | 0.46 | 0.47 | 0.34 | 0.62 | 0.81 | 0.69 | 0.33 | 0.34 | 0.52 |
| Total | 98.19 | 98.01 | 99.64 | 100.05 | 99.89 | 99.68 | 99.85 | 102.58 | 99.81 |

| | 10 | 11 | 12 | 13 | 14 | 15 | 16 | 17 | 18 |
|---|---|---|---|---|---|---|---|---|---|
| | 10-4b | 222/420k | 222/420b | 222/403k | 218/415k | 222/437b | 03-180/450b | 03-179/450b | 222/467k |
| $SiO_2$ | 28.32 | 30.8 | 31.5 | 31.25 | 28.4 | 29.51 | 29.79 | 27.02 | 30.71 |
| $TiO_2$ | 1.34 | 1.65 | 1.58 | 1.44 | 1.93 | 1.35 | 1.49 | 1.08 | 1.89 |
| $Al_2O_3$ | 1.97 | 2.5 | 2.13 | 2.40 | 2.7 | 3.30 | 2.39 | 1.70 | 3.21 |
| $Fe_2O_3$ | 3.42 | 2.74 | 2.56 | 2.64 | 3.64 | 4.05 | 2.87 | 2.97 | 3.88 |
| FeO | 5.64 | 7.45 | 7.25 | 6.70 | 6.00 | 6.20 | 5.63 | 4.81 | 6.35 |
| MnO | 0.17 | 0.17 | 0.15 | 0.15 | 0.19 | 0.19 | 0.14 | 0.14 | 0.20 |
| MgO | 30.98 | 33.56 | 35.48 | 34.64 | 31.85 | 30.38 | 29.36 | 31.56 | 30.49 |
| CaO | 13.46 | 11.22 | 9.25 | 11.77 | 13.64 | 14.11 | 10.56 | 14.34 | 13.02 |
| $Na_2O$ | 0.28 | 2.63 | 1.83 | 0.38 | 0.88 | 0.62 | 3.10 | 0.19 | 2.82 |
| $K_2O$ | 1.16 | 0.78 | 0.81 | 0.57 | 1.03 | 1.14 | 2.07 | 0.72 | 0.75 |
| $H_2O$ | 2.11 | 0.94 | 0.59 | 1.85 | 0.76 | 0.65 | 4.19 | 3.97 | 0.54 |
| $CO_2$ | 9.89 | 4.73 | 5.83 | 5.72 | 8.36 | 8.34 | 7.04 | 9.52 | 5.38 |
| $P_2O_5$ | 0.56 | 0.53 | 0.33 | 0.47 | 0.51 | 0.51 | 0.39 | 0.47 | 0.63 |
| F | 0.16 | 0.09 | 0.06 | 0.09 | 0.23 | – | 0.22 | 0.22 | – |
| Cl | 0.38 | – | – | – | – | – | – | – | – |
| Total | 99.84 | 99.79 | 99.35 | 100.07 | 100.12 | 100.35 | 99.23 | 98.71 | 99.87 |

| | 19 | 20 | 21 | 22 | 23 | 24 | 25 | 26 | 27 |
|---|---|---|---|---|---|---|---|---|---|
| | 222/471k | 222/476k | 222/489k | 222/504b | 08-11b | 07-5k | 03\33k | 03\91k | 03\101k |
| $SiO_2$ | 30.19 | 33.3 | 26 | 25.48 | 28.89 | 28.56 | 27.79 | 28.74 | 28.10 |
| $TiO_2$ | 1.78 | 1.9 | 1.34 | 1.45 | 1.569 | 0.957 | 1.53 | 1.29 | 2.91 |
| $Al_2O_3$ | 2.46 | 2.88 | 2.43 | 2.43 | 2.11 | 2.39 | 1.52 | 1.77 | 1.78 |
| $Fe_2O_3$ | 3.11 | 1.9 | 1.8 | 3.15 | 3.77 | 3.41 | 3.64 | 4.94 | 5.22 |
| FeO | 7.44 | 7.9 | 5.1 | 5.45 | 5.28 | 4.54 | 5.50 | 4.08 | 5.39 |
| MnO | 0.19 | 0.16 | 0.12 | 0.17 | 0.142 | 0.129 | 0.17 | 0.18 | 0.18 |
| MgO | 31.69 | 35.9 | 27.04 | 28.96 | 31.71 | 29.09 | 31.76 | 31.90 | 30.63 |

(continued)

**Table 2** (continued)

| | 19 | 20 | 21 | 22 | 23 | 24 | 25 | 26 | 27 |
|---|---|---|---|---|---|---|---|---|---|
| | 222/471k | 222/476k | 222/489k | 222/504b | 08-11b | 07-5k | 03\33k | 03\91k | 03\101k |
| CaO | 13.43 | 8.86 | 18.06 | 15.67 | 13.41 | 15.41 | 13.75 | 11.20 | 11.70 |
| $Na_2O$ | 0.39 | 0.4 | 0.07 | 0.09 | 0.27 | 0.49 | 0.12 | 0.08 | 0.09 |
| $K_2O$ | 0.95 | 0.49 | 1.63 | 1.93 | 1.273 | 1.289 | 0.92 | 0.82 | 1.06 |
| $H_2O$ | 0.58 | 2.55 | 2.88 | 2.01 | 0.93 | 0.81 | 1.82 | 5.49 | 3.69 |
| $CO_2$ | 7.39 | 3.19 | 12.54 | 13.20 | 9.6 | 10.25 | 9.57 | 7.59 | 7.59 |
| $P_2O_5$ | 0.42 | 0.40 | 0.31 | 0.50 | 0.397 | 0.334 | 0.66 | 0.55 | 0.45 |
| F | – | 0.13 | 0.10 | – | 0.19 | 0.34 | 0.27 | 0.17 | 0.15 |
| Cl | – | – | – | – | 0.39 | – | – | – | 0.47 |
| Total | 100.02 | 99.96 | 99.42 | 100.49 | 99.93 | 98.19 | 99.02 | 98.80 | 99.41 |
| | 28 | 29 | 30 | 31 | 32 | 33 | 34 | 35 | 36 |
| | 03\142k | 03\164k | 04-114 k | 222/A-1 | 222/A-8 | Eg-Phl | Eg-j | Middle 34an | 10-10 |
| $SiO_2$ | 27.80 | 32.18 | 26.04 | 26.60 | 31.75 | 35.59 | 31.50 | 28.73 | 27.32 |
| $TiO_2$ | 1.84 | 1.29 | 1.08 | 1.83 | 1.45 | 4.47 | 1.50 | 1.65 | 1.23 |
| $Al_2O_3$ | 1.66 | 1.54 | 1.51 | 2.32 | 2.72 | 3.2 | 2.05 | 2.22 | 1.95 |
| $Fe_2O_3$ | 3.83 | 3.11 | 3.52 | 2.47 | 3.46 | 4.24 | 3.14 | 3.52 | 4.56 |
| FeO | 6.12 | 6.17 | 4.90 | 5.55 | 5.75 | 7.65 | 7.50 | 5.72 | 2.96 |
| MnO | 0.16 | 0.17 | 0.14 | 0.14 | 0.17 | 0.19 | 0.16 | 0.16 | 0.13 |
| MgO | 30.52 | 36.37 | 31.50 | 28.22 | 34.68 | 24.45 | 33.58 | 31.00 | 30.56 |
| CaO | 12.37 | 7.47 | 16.15 | 16.4 | 9.39 | 10.01 | 12.44 | 13.39 | 10.36 |
| $Na_2O$ | 1.91 | 0.67 | 0.26 | 0.17 | 0.19 | 2.53 | 0.28 | 0.74 | 0.72 |
| $K_2O$ | 1.16 | 1.40 | 0.68 | 1.42 | 1.25 | 2.87 | 0.92 | 1.13 | 0.54 |
| $H_2O$ | 2.44 | 2.96 | 0.70 | 2.72 | 1.54 | 2.88 | 0.87 | 2.01 | 10.48 |
| $CO_2$ | 8.22 | 4.88 | 11.41 | 11.00 | 7.00 | 1.83 | 5.43 | 8.53 | 7.90 |
| $P_2O_5$ | 0.54 | 0.42 | 0.43 | 0.45 | 0.43 | 0.07 | 0.36 | 0.47 | 0.38 |
| F | 0.17 | 0.30 | 0.18 | 0.10 | 0.10 | 0.04 | 0.08 | 0.15 | 0.14 |
| Cl | 1.53 | 1.11 | 0.44 | – | – | – | – | | 2.23 |
| Total | 98.74 | 98.93 | 98.51 | 99.39 | 99.88 | 100.02 | 99.81 | 99.42 | 99.23 |

*Comment* In sample numbers, the last letter refers to kimberlite breccia (*b*), phase 1 hypabyssal kimberlite (*k*), hypabyssal kimberlite of late dykes (*d*), – not analyzed

values (0.712052) are measured in coarse halite in geodes (Table 4).

## Discussion

### Contrasts in Southern and Northern Yakutian Kimberlites

The mineralogy and genesis of the serpentine-free Udachnaya kimberlite cannot be understood without data on geology and country rocks of Yakutian kimberlites in general. As kimberlite is a hybrid rock, its composition is affected by lithology of the host country rocks (Mitchell 1986). Classical southern African kimberlites erupt through dolerites, quartz sandstones, and crystalline basement (Field and Scott Smith 1999) and show relatively low contents of CaO and $CO_2$ (Fig. 9a). The Archangelsk kimberlites that erupt through sandstones contain no more than 5 wt.% $CaCO_3$ (Fig. 9a). In this context, the average content of 23.6 wt.% CaO in Yakutian kimberlites is exceptional and relates to emplacement through and contamination by terrigenous carbonate sediments (Khar'kiv et al. 1991; Kostrovitsky 1986). Compared to other economic kimberlites, Yakutian kimberlites have incorporated distinctly more carbonate-rich country rock xenoliths (assessed as 15–20 vol %; Khar'kiv et al. 1991). In addition to high and variable CaO and $CO_2$ bulk contents in Yakutian kimberlites, the carbonate-rich country rocks bring about a very broad range of $\delta^{13}C$ values and higher positive $\delta^{18}O$ (Fig. 9b). When separated by the thickness of the sedimentary cover into northern and southern Yakutian

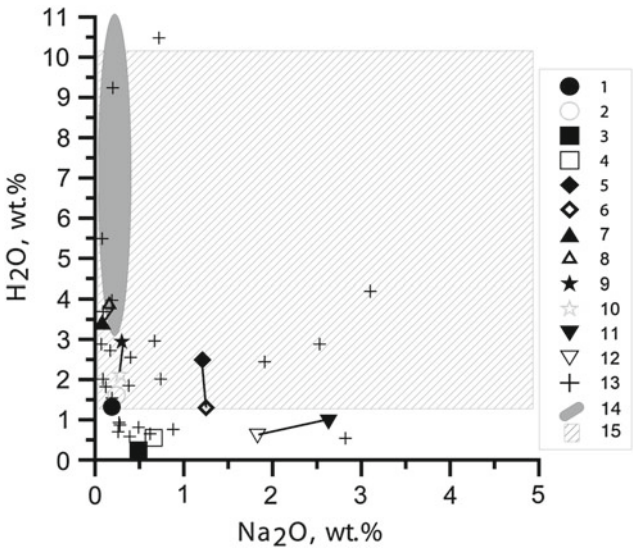


**Fig. 7** A plot of $Na_2O$ versus $H_2O$ for SFUE kimberlites. Symbols connected by *tie-lines* show compositions of distinct kimberlite phases in composite specimens represented by either clasts of hypabyssal kimberlite in breccia, or breccia cut by late hypabyssal dykes. *1*, *3*, *5*, *7*, *9*, *11* hypabyssal kimberlite of the clasts and the dykes; *2*, *4*, *6*, *8*, *10*, *12* kimberlite breccia (see Table 1); *13* non-composite SFUE kimberlites; *14* Slave kimberlites (Kopylova and Hayman 2008); *15* Yakutian kimberlites (Khar'kiv et al. 1991)

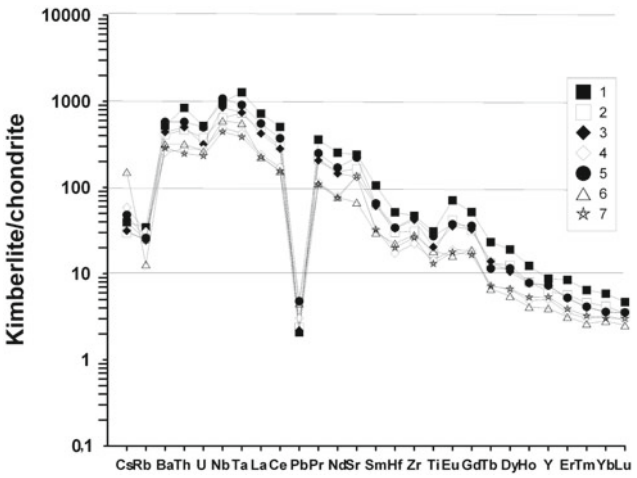


**Fig. 8** Trace element concentrations in the Udachnaya-East kimberlite normalized to chondrite abundances (McDonough and Sun 1995). *Symbols 1* sample 10-4 HK, *2* sample 10-4 breccia, *3* sample 07-6 HK, *4* sample 07-6 breccia, *5* sample 03-142 PK, *6* sample 08-3 breccia, *7* sample 07-5 breccia

kimberlites, these two divisions demonstrate contrasting C and O isotope ratios. Northern kimberlites plot around the worldwide Group I kimberlites and incorporate values for magmatic carbonate, whereas southern kimberlites shift to higher values of $\delta^{18}O$ (15–23 ‰) and a broader range in $\delta^{13}C$. The systematics of the O–C isotopes can be explained by mixing of mantle melts with modern and ancient sedimentary carbonates (Fig. 9b).

Sedimentary carbonates in the local Paleozoic stratigraphy are accompanied by evaporite beds and strata of various lithologies saturated with ancient waters and brines. Mixing of country rock evaporites and groundwaters into kimberlites can be traced geochemically by elevated Cl, Na, and S. Southern Yakutian pipes (fields 1–4 in Fig. 1) are uniquely high in Cl and S contents. For example, sulfur is elevated in Mir, Udachnaya, and International'naya kimberlites (0.8–5.3 wt.%), but is low (0–0.3 wt.%) in northern Yakutian pipes (Khar'kiv et al. 1991), as it is in typical kimberlites worldwide. The average Cl content in Indian and African kimberlites is 0.03–0.06 wt.% (Ilupin et al. 1978), which is 10–100 times lower than that in the SFUE kimberlite (Tables 1, 2). Southern Yakutian kimberlites also demonstrate elevated $Na_2O$ content, up to 5 wt.%, much higher than other worldwide kimberlites, exemplified by the Slave Craton kimberlites on Fig. 7. The halite abundance and spatial distribution match the lithology of country rocks at the corresponding levels. For example, the highest (8 vol %) abundance of halite is restricted to depth levels of southern diatremes (Mir, Udachnaya, and International'naya) where they cut through halite-rich evaporite. This is also true for gypsum and anhydrite (Khar'kiv et al. 1991).

## Petrographic and Geochemical Evidence for Crustal Contamination of the SFUE Kimberlite

Mineralogical mapping of the Udachnaya-East pipe shows that the highest abundances of Na–Cl–S-bearing minerals occur at a depth interval that transcends 3 magmatic phases of kimberlites formed at different times from different magma batches (Fig. 2). This unequivocally suggests a secondary origin for the Na–Cl–S-bearing minerals. A secondary origin is also supported by the textural relationships of halite and alkali carbonate to serpentine and other groundmass minerals as observed in thin sections (Pavlov and Ilupin 1973; Egorov et al. 1988; Kornilova et al. 1998). Furthermore, halite, gypsum, and carbonate are present not only in veins cutting through kimberlite and xenoliths (Egorov et al. 1988; Sharygin et al. 2007a, b; Polozov et al. 2008a), but also in modern brine deposits in the pipe and in the secondary geodes (Fig. 4).

The secondary nature of the Na–Cl–S mineralization is also suggested by our observation that contents of $Na_2O$ and $H_2O$ are a function of the spatial position of the kimberlite specimen in the pipe (Fig. 9) rather than the melt compositions of distinct magma batches. Moreover, we found that the inverse correlation between $H_2O$ and $Na_2O$ demonstrated on Fig. 1 of Kamenetsky et al. (2009b) disappears if the data are plotted on a linear rather than on a logarithmic scale. Our analyses of the Udachnaya-East kimberlite show no inverse correlation between $H_2O$ and $Na_2O$ (Fig. 9). The absence of

**Table 3** Rare element composition (in ppm) of SFUE kimberlites

| | 03-142 k | 07-6d | 07-6b | 10-4d | 10-4b | 08-3b |
|---|---|---|---|---|---|---|
| Li, ppm | – | – | – | 22 | 14.3 | |
| Be | 1.54 | 1.37 | 1.08 | 2.25 | 1.81 | 1.21 |
| Sc | 12.0 | 11.5 | 6.5 | 18 | 11.4 | 8.6 |
| V | 143 | 91 | 88 | 137 | 104 | 98 |
| Cr | 1,244 | 1,266 | 706 | 2,186 | 1,261 | 968 |
| Co | 67 | 67 | 52 | 76 | 81 | 28.5 |
| Ni | 885 | 939 | 817 | 801 | 1154 | 844 |
| Cu | 64.9 | 50.6 | 36.5 | 60 | 60 | 0.95 |
| Zn | 68 | 67 | 51 | 72 | 59 | 8.7 |
| Ga | 3.54 | 3.92 | 2.56 | 7.0 | 3.97 | 2.92 |
| Ge | 0.8 | 0.72 | 0.63 | 0.69 | 0.71 | 0.83 |
| Rb | 59.6 | 55.8 | 71.3 | 79 | 59 | 29.5 |
| Sr | 1,617 | 964 | 979 | 1,745 | 1,194 | 486 |
| Y | 11.5 | 11.5 | 7.9 | 13.7 | 9.8 | 6.2 |
| Zr | 169 | 160 | 85 | 179 | 119 | 107 |
| Nb | 258 | 203 | 118 | 232 | 153 | 143 |
| Mo | 2.22 | 0.43 | 0.55 | 1.47 | 1.10 | 1.58 |
| Sn | 1.78 | 1.45 | 1.22 | 1.56 | 1.08 | 1.01 |
| Cs | 0.91 | 0.6 | 1.11 | 0.75 | 0.56 | 2.88 |
| Ba | 1,391 | 1,059 | 619 | 1,258 | 983 | 768 |
| La | 131 | 100 | 57 | 171 | 109 | 53 |
| Ce | 228 | 173 | 105 | 310 | 185 | 95 |
| Pr | 23.2 | 19.2 | 10.7 | 33 | 20 | 10.3 |
| Nd | 77.8 | 66.5 | 36 | 116 | 70 | 35.1 |
| Sm | 9.7 | 9.0 | 4.8 | 16 | 9.3 | 4.4 |
| Eu | 2.1 | 1.98 | 1.06 | 3.94 | 2.36 | 0.90 |
| Gd | 7.1 | 6.5 | 3.7 | 12.0 | 7.0 | 3.7 |
| Tb | 0.41 | 0.5 | 0.26 | 0.98 | 0.79 | 0.24 |
| Dy | 2.83 | 2.58 | 1.62 | 4.70 | 3.08 | 1.35 |
| Ho | 0.43 | 0.42 | 0.27 | 0.67 | 0.44 | 0.22 |
| Er | 0.84 | 0.83 | 0.56 | 1.35 | 0.91 | 0.50 |
| Tm | 0.1 | 0.1 | 0.07 | 0.16 | 0.11 | 0.07 |
| Yb | 0.58 | 0.58 | 0.52 | 0.94 | 0.67 | 0.45 |
| Lu | 0.09 | 0.09 | 0.07 | 0.11 | 0.085 | 0.06 |
| Hf | 3.51 | 3.44 | 1.78 | 5.3 | 3.1 | 2.31 |
| Ta | 12.4 | 10.1 | 5.82 | 17 | 10.0 | 7.60 |
| W | 6.65 | 1.99 | 0.81 | 2.43 | 1.47 | 1.57 |
| Pb | 11.8 | 5.41 | 7.5 | 5.2 | 5.9 | 11.2 |
| Th | 16.7 | 14.5 | 8.07 | 24 | 13.6 | 9.3 |
| U | 3.7 | 2.36 | 2.07 | 3.83 | 2.8 | 1.95 |

*Comment* In sample numbers, the last letter refers to kimberlite breccia (*b*), phase 1 hypabyssal kimberlite (*k*), hypabyssal kimberlite of late dykes (*d*)

any correlation between $Na_2O$ and $H_2O$ in Udachnaya-East is typical of kimberlites in general, including kimberlites that contain unserpentinized macrocrysts and phenocrysts of olivine. Such samples are rare in Siberia, but common worldwide (Scott Smith 1996; Kopylova and Hayman 2008). These fresh kimberlites have no more than 0.2 wt.% $Na_2O$,

**Table 4** Major, trace element and Sr–Nd isotopic composition of salts in the SFUE kimberlite

| Sample no. | Salt recently deposited in the open pit | Halite xenoliths | Geode with coarse halite and sylvine in SFUE |
|---|---|---|---|
| | 08-21 | 10-10 Na | 10-22 |
| Mg, wt.% | 0.287 | 0.36 | 0.215 |
| Al | 0.0073 | 0.039 | 0.033 |
| Si | 0.12 | 0.241 | 0.171 |
| NaCl | 99.25 | 98.18 | 95.66 |
| K | 0.0459 | 0.03 | 3.41 |
| Ca | 0.246 | 0.616 | 0.224 |
| Fe | 0.0154 | 0.0578 | 0.0753 |
| Br | 0.0283 | 0.0342 | 0.041 |
| S | – | 0.386 | 0.0011 |
| Sr, ppm | 21 | 140 | 11 |
| Rb, ppm | 0.39 | 0.64 | 6.8 |
| $^{87}Rb/^{86}Sr$ | 0.05374 | 0.01323 | 1.79268 |
| $(^{87}Sr/^{86}Sr)_i$ | 0.708348 | 0.708227 | 0.72205 |
| $\varepsilon Sr_i$ | 54.6 | 59 | 255.3 |
| Age (Ma) | 0 | 360 | 360 |

while $H_2O$ contents vary independently from 3.8 to 10.7 wt.% (Fig. 9). The absence of $Na_2O$–$H_2O$ correlation is supported by findings of kimberlite with serpentinized olivine that contains halite in the groundmass and halite xenoliths. For example, in sample 10-10 (Table 2), high $H_2O$ content (10.48 wt.%) is accompanied by high (0.74 % wt.%) $Na_2O$, implying a significant mode of halite in the matrix. This evidence demonstrates that Na-rich kimberlite compositions are not solely restricted to unserpentinized kimberlites and that groundmass serpentine does not replace primary alkali- and chlorine-bearing minerals.

The strongest evidence for the secondary origin of Na-, Cl-, and S-rich minerals in the Udachnaya-East kimberlite and in all southern Yakutian kimberlites, in our opinion, is the regional correlation between the geology and hydrogeology of the local country rocks and the mineralogy of Yakutian kimberlites, in particular the difference between southern and northern kimberlites. Na–Cl–S mineralization is more significant for southern kimberlites that erupt through the thicker, evaporite-bearing sequence of carbonate sediments (Fig. 2b).

## Isotopic Evidence for Crustal Contamination of the SFUE Kimberlite

Values of C and O isotopic ratios for the Udachnaya-East kimberlite were reported by Egorov et al. (1986), Kostrovitsky (1986), and Khar'kiv et al. (1991, 1998). Carbon isotopic ratios in SFUE kimberlite plot among the highest values in the field of contaminated Yakutian kimberlites (Fig. 9b). Isotopic compositions of C (−3.4 to −0.8 ‰ $\delta^{13}C$) are heavier than those of the mantle and require mixing with sedimentary marine carbonates (Fig. 9b) that may have been sourced from country rock carbonate xenoliths. Isotopic compositions of O vary from 15.36 to 18.59 ‰ $\delta^{18}O$, which is between the mantle (+8 ‰) and the marine sedimentary (+22 ‰) values. Both C and O isotopes of the Udachnaya-East kimberlite thus reflect mixing of a mantle melt with crustal carbonates.

The same conclusion was reached by Khar'kiv et al. (1991). The Udachnaya-East kimberlite has $\delta^{13}C$ equal to (−3.4)–(−2.7) ‰ at 20–400 m, (−1.6)–(−1.3) ‰ at 400–600 m, and (−1.5)–(−2.1 ‰) at 600–900 m (Khar'kiv et al. 1991). The highest $\delta^{13}C$ values are observed at the depth where SFUE kimberlite occurs, suggesting the most significant contamination by heavy crustal carbon at 400–600 m.

Sulfur isotopes in southern Yakutian kimberlites are characterized by high $\delta^{34}S$ (15–53 ‰) (Fig. 10). Mantle samples and magmas, including kimberlites, generally plot around $\delta^{34}S = 0$ ‰, but the Udachnaya $\delta^{34}S$ values are closer to that of the local sedimentary rocks. Another study of sulfur isotopes in sulfate minerals in the southern Yakutian kimberlites (Ilupin et al. 1978) also indicates a sedimentary source of sulfur.

Chlorine isotopic ratios of halite in SFUE kimberlite (−0.25 to 0.4 ‰ $\delta^{37}Cl$, Sharp et al. 2007) are consistent with evaporites (−0.5 to 0.5 ‰ $\delta^{37}Cl$) and Udachnaya brines (−0.33 to 0.52 ‰, Alekseev et al. 2007).

Strontium isotopic ratios measured for different kimberlite minerals and rock components constrain the history of kimberlite crystallization. Sr isotopic ratios ($^{87}Sr/^{86}Sr_i$) of the SFUE megacrystic clinopyroxene and groundmass perovskite are 0.70292–0.70308 (Kamenetsky et al. 2009b). These values are much lower than Sr isotopic ratios of the bulk Udachnaya kimberlite, water, and acid leachates (Maas et al. 2005; Kamenetsky et al. 2009b). The difference $\Delta^{87}Sr/^{86}Sr_i$ of up to 0.006 between the bulk kimberlite Sr ratios (0.7033–0.709; Kostrovitsky 1986; Kornilova et al. 1998; Kostrovitsky et al. 2007; Maas et al. 2005; Fig. 11) and those of the kimberlite minerals exceeds that for other kimberlites, reflecting a particularly complex history of crustal contamination of the Udachnaya kimberlite. Typically, Sr ratios of the bulk kimberlite are 0.001–0.0053 higher than those of perovskite and megacrysts (Paton et al. 2007; Kostrovitsky et al. 2007; Kopylova et al. 2009; Woodhead et al. 2009).

The $^{87}Sr/^{86}Sr_i$ values in bulk SFUE kimberlite are 0.70438–0.709, which are higher than those in Group I kimberlites (Fig. 11). These values do not include analyses

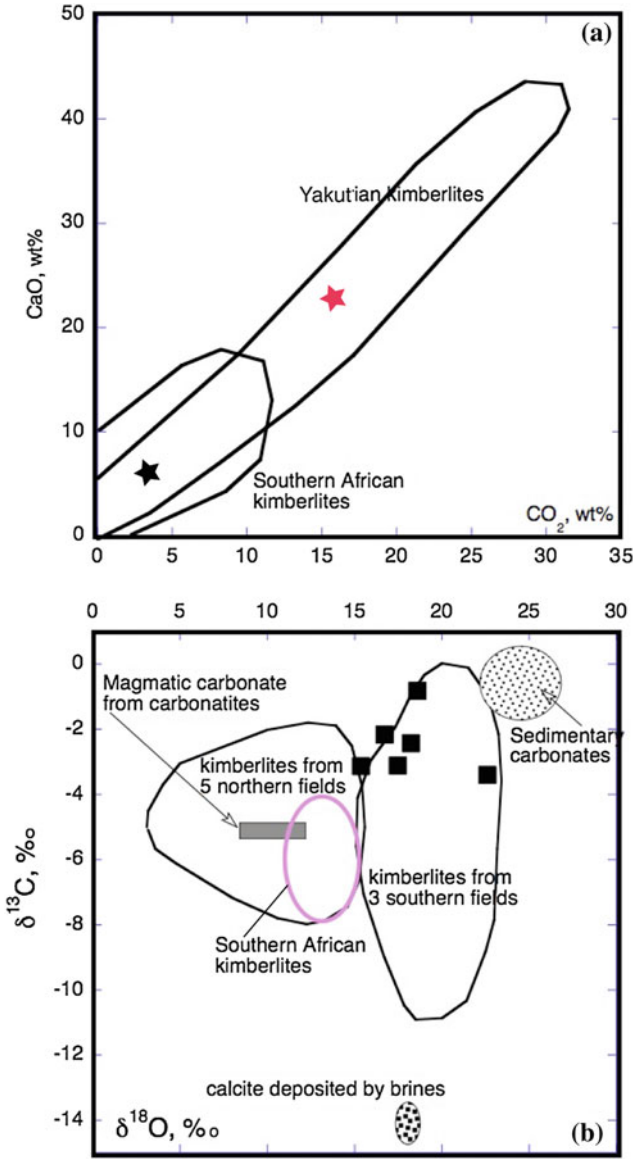


**Fig. 9** Compositions of Yakutian kimberlites, modified after Khar'kiv et al. (1991). **a** A CaO–$CO_2$ (wt.%) plot. The average contents of these oxides in Yakutian kimberlites (*red star*) are calculated for 171 analyses. The average for the Archangelsk kimberlites (*black star*) is from Bogatikov et al. (1999). **b** A plot of O and C isotopes in the SFUE kimberlite in comparison with data on Yakutian and southern African kimberlites and carbonates in various rock types. Isotopic ratios for SFUE kimberlite (Egorov et al. 1986) are denoted as *black squares*

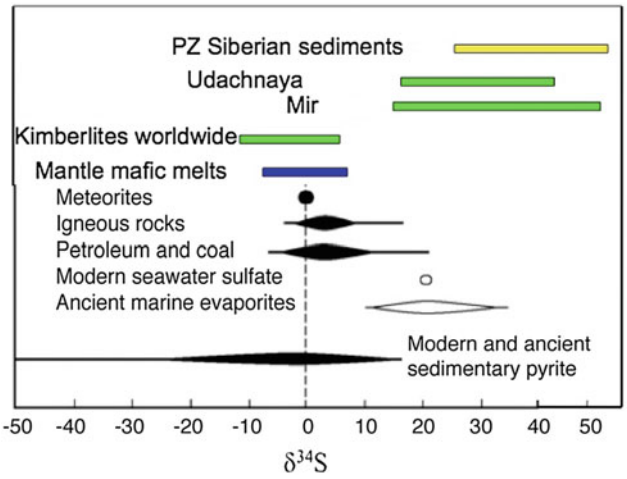


**Fig. 10** Stable isotope ratio $\delta^{34}S$ for various terrestrial rocks and minerals (Seal 2006), southern Yakutian kimberlites, and their country rock sediments (Vinogradov and Ilupin 1972)

of salts, water-soluble fraction of the SFUE kimberlite, and acid leachates that yielded "unrealistically" low initial $^{87}Sr/^{86}Sr$ ratio (<0.700) (Maas et al. 2005), in the authors' words. The highest $(^{87}Sr/^{86}Sr)_i$ ratio of 0.709 is observed in the bulk sample with the most intense development of secondary carbonate. The Sr isotopes reflect the mixture of the kimberlite with Udachnaya brines ($^{87}Sr/^{86}Sr_i = 0.7088 - 0.7092$, Alekseev et al. 2007) or halite xenoliths (0.707871, Table 4). εNd of the SFUE kimberlite is 2–4 (Maas et al. 2005), typical of the asthenospheric magmas, including Group I kimberlites. As Nd isotopes are not affected by crustal carbonate contamination (Kostrovitsky et al. 2007), mantle values of Nd ratios in the SFUE kimberlite cannot be used as an argument for a pristine mantle origin.

## The Origin of Na–Cl–S Minerals in the SFUE Kimberlite

The contamination of the SFUE kimberlite and other southern Yakutian kimberlites by Na–Cl–S crustal material occurred, in our opinion, in two different ways. The kimberlites may have been contaminated by buried brines. The upper contact of the SFUE kimberlite coincides with the roof of the deep Udachnaya aquifer, with a high hydraulic pressure and anomalously Na-rich brines. The Udachnaya pipe is on the boundary between strata saturated with Na–Cl and Ca–Cl brines. The western part of the pipe was penetrated by Ca–Cl brines, whereas the eastern part of the pipe at the same depth is inundated by Na–Cl brines. It is possible that this hydrogeological feature controlled formation of the SFUE kimberlite with high modes of Na-, Cl-, and S-bearing minerals. It is these brines that precipitate halite in the Udachnaya-East open pit and leach solid, fully crystallized kimberlite producing cavities and geodes with Na–Cl–S minerals (Fig. 4). It was shown experimentally that even short (2–6 days) contact of kimberlite with brines changes its composition (Khar'kiv et al. 1991).

The second possible origin of extraneous Cl, S, and alkalies may be assimilation of carbonate-, sulfate-, and chloride-rich country rock xenoliths. Large xenoliths of halite found in the kimberlite were likely sourced from the

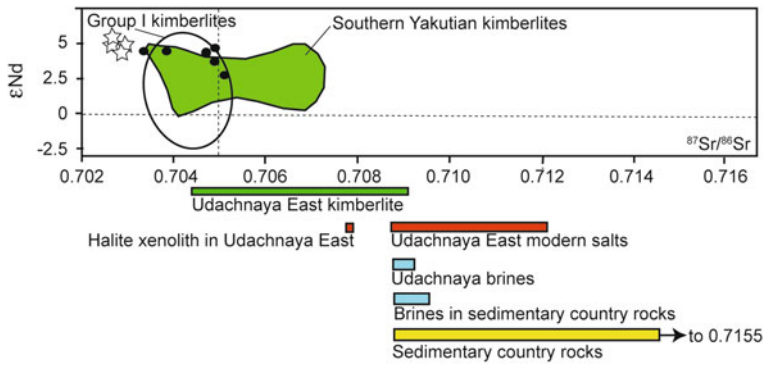


**Fig. 11** Initial ratios of Sr and Nd isotopes for Group I and southern Yakutian kimberlites. Open stars mark compositions of perovskite and a clinopyroxene megacryst from the SFUE kimberlite (Kamenetsky et al. 2009b). *Bars below* the Sr–Nd plot indicate bulk Sr compositions of the Udachnaya kimberlite (Maas et al. 2005; Kamenetsky et al. 2009b; Kostrovitsky et al. 2007), halite xenoliths and modern salts (Table 4), sedimentary country rocks of the Udachnaya pipe (Kononov 2009), and Udachnaya brines (Alekseev et al. 2007; Kononov 2009)

Middle Cambrian Chukuck suite of the Daldyn-Markha bank. The xenoliths cannot be late chloride-rich segregations from a residual kimberlite melt (Kamenetsky et al. 2007b) as they have thermally metamorphosed margins (Polozov et al. 2008a, b) and angular shapes (Fig. 6). The contrasting compositions of evaporites and kimberlite melt should cause skarn-like exchange of components on contacts between xenoliths and kimberlite. Similar zones of mini-skarns are observed on contacts of felsic xenoliths with kimberlites, introducing elements enriched in xenoliths to kimberlite and leading to pervasive crystallization of hybrid minerals (Caro et al. 2004). Assimilation of evaporite xenoliths occurs at relatively high, magmatic temperatures producing hybrid melt with elevated contents of Na, K, Cl, and S. This melt is trapped as Cl-rich fluid inclusions in secondary fractures of olivine (Golovin et al. 2003). Alkali-, sulfur-, and chlorine-rich minerals may have crystallized from this late hybrid melt and may be "comagmatic" with kimberlite, as found by Maas et al. (2005).

## The Relationship Between Serpentinization and Na–Cl–S Mineralization

The reason for a serpentine-free character of some Udachnaya-East kimberlite rich in Na, Cl and S minerals is not fully understood. Serpentine in kimberlites has a variety of origins, depending on its textural position. Interstitial serpentine of the groundmass may be magmatic (Scott Smith 1996) crystallizing at $T > 600$ °C (Kopylova et al. 2007). Serpentine replacing monticellite and olivine rims may be deuteric ($T > 300$ °C, Mitchell 2006), and serpentine replacing large olivine may have formed after the emplacement from meteoric groundwaters.

The absence of all textural types of serpentine in SFUE kimberlite is easily explained by the model of the evaporite country rock contamination. The hybrid residual kimberlite melt that digested evaporite xenoliths had lower $H_2O$ activity due to increased halogen and alkali abundances (e.g., Aranovich and Newton 1996). It has been found that the solubility of $H_2O$ in haplogranite melt decreases from 5 to 3.5 wt.% with increasing concentrations of alkali chlorides in the aqueous fluid (Fig. 2B of Webster 1992). Chlorine solubility in carbonate-rich melts is unknown, but when Cl concentrations in a melt reach the critical minimum amount required for exsolution of hydrosaline chloride fluid, the fluid removes $H_2O$ from the melt completely (Aiuppa et al. 2009). High-salinity fluids reduce the stability field of serpentine (Sharp and Barnes 2004) so that the melt is expected to form late interstitial alkali carbonates and chlorides instead of serpentine. The absence of serpentinization of olivine macrocrysts is also controlled by the less hydrous composition of residual melts and deuteric fluids. Low-P crystallization experiments on kimberlites demonstrated that at 895 °C, forsterite peritectically reacts with the residual melt saturated with $H_2O$ and $CO_2$ (Franz and Wyllie 1967). The absence of carbonatitic hydrous reactive melt would hinder the peritectic reaction and keep olivine intact. Experiments on crystallization of K-rich melts also show that in the absence of water, olivine is stable to lower temperatures (by 50–150 °C, Fig. 11 of Yoder 1986) than in the respective wet composition. Moreover, it has been observed that olivine is fresher in calcite-rich kimberlites (Mitchell, personal communication), again emphasizing the critical role of deuteric fluid composition on the kimberlite mineralogy.

A model of the SFUE kimberlite origin due to a reaction with buried brines explains the fresh character of olivine by the impeded serpentinization. Experiments on interaction between a solid kimberlite and meteoric water with elevated Na and Cl contents at room temperatures demonstrated that such water cannot serpentinize olivine (Lashkevich and Egorov 1988). This effect was also modeled for abyssal peridotites (Novoselov 2010). This model, however, cannot

explain the absence of magmatic serpentine that crystallizes as late groundmass mineral in fresh kimberlites. For this phenomenon, we propose a uniquely low $H_2O$ content (<0.5–1.0 %) for the Udachnaya-East primary kimberlite melt. The observed $H_2O$ contents of up to 5.5 % in the SFUE kimberlite (Table 2) may be secondary, similar to the $Na_2O$ contents, as evidenced by the spatial control on the $H_2O$ and $Na_2O$ concentrations (Fig. 7).

## Do Melt and Fluid Inclusions in Olivine and Fibrous Diamond Prove the Mantle Origin of Chlorides in Kimberlites?

Melt inclusions in kimberlitic olivines with chloride- and carbonate-rich composition (Golovin et al. 2003, 2007; Sharygin et al. 2007a, b) and alkali- and Cl-rich fluid inclusions in fibrous diamonds were cited (Kamenetsky et al. 2004) as evidence for the mantle origin of chlorides in kimberlites. Below we present a critique of these statements.

Chloride-and alkali-rich melt inclusions in kimberlitic olivines may not imply the mantle source of Cl, Na, and K, as the inclusions are found only in olivine microfractures and are clearly secondary (Golovin et al. 2003, 2007). The inclusions trapped by thermally and explosively cracked olivines supply information on late residual melts and fluids equilibrated with kimberlite melts in the subsurface. Compositions of these inclusions contrast to primary deep-seated $CO_2$-rich inclusions in Udachnaya olivine (Sobolev et al. 1989). Furthermore, secondary composite melt/fluid inclusions in Udachnaya olivines differ significantly from those in the Slave and Greenland kimberlitic olivines. The former are distinctly higher in (Na + K)/(Na + Ca + K) (Fig. 8A of Kamenetsky et al. 2009a). Only the Udachnaya olivine inclusions contained anhydrous carbonates or sulfates, whereas inclusions in all other studied kimberlites worldwide hosted hydrated carbonates and sulfates indicating a greater amount of water in residual magmas (Mernagh et al. 2012). The distinct mineralogy and composition of the secondary fluid inclusions in Udachnaya-East imply a unique process of late, subsurface $H_2O$ depletion and Na enrichment.

The similarity between compositions of fluid inclusions in fibrous diamonds and constrained alkali-rich composition of primary kimberlite melt (Fig. 3 of Kamenetsky et al. 2004) is fictitious. The conventional representation of the compositional data in the (K + Na)–Ca–Si triangle plots all alkalis together and masks significant differences between Na-rich Udachnaya compositions (Table 2) and K-rich diamond inclusions (e.g., Klein-BenDavid et al. 2009). Moreover, the sulfur-rich character of the Udachnaya kimberlite (Khar'kiv et al. 1991) does not have parallels with mantle fluids or diamond fluid inclusions.

## Conclusions

SFUE kimberlite and other kimberlites of southern Yakutian fields rich in halite, alkali carbonate, gypsum, and other salts acquired the high Na, S, and Cl contents by interaction with buried Cambrian Na–Ca–Cl brines or assimilating evaporite xenoliths. The classic view of kimberlites as $Na_2O$-poor rocks with high K/Na ratios (Dawson 1980; Mitchell 1986) remains unchanged.

**Acknowledgments** The studies were supported by the integration projects of the Russian Academy of Sciences № 59, 115, and 27.1 and by an NSERC Discovery Grant to MGK. The authors thank G. Sandimirova and Yu. Pakhol'chenko for isotopic analyses, A. Polozov for helpful discussions, and E. Smith for the editorial help.

## References

Aiuppa A, Baker DR, Webster JD (2009) Halogens in volcanic systems. Chem Geol 263:1–18

Alekseev SV, Alekseeva LP, Borisov VN, Shoukar-Stash O, Frape SK, Chabaux F, Kononov AM (2007) Isotopic composition (H, O, Cl, Sr) of ground brines of the Siberian platform. Russ Geol Geophys 48:225–236

Aranovich LY, Newton RC (1996) $H_2O$ activity in concentrated NaCl solutions at high pressures and temperatures measured by the brucite-periclase equilibrium. Contrib Mineral Petr 125(2–3): 200–212

Bobrievich AP, Bondarenko MN, Gnevushev MA, Krasov LM, Smirnov GI, Yurkevich RK (1959) Diamondiferous deposits of Yakutia. State scientific-techniques publishing house, Moskow, p 527 (in Russian)

Bogatikov OA, Garanin VK, Kononova VA, Kudryavtceva GP, Vasil'eva EP, Verjak VV, Verichev EM, Posuhova TV (1999) The Arkhangelsk diamondiferous province (geology, petrography, geochemistry and mineralogy). MGU, Moskow, p 524

Brakhfogel FF (1984) Geological aspects of kimberlite magmatism in the north-east of the Siberian platform. Yakutsk, USSR, p 128 (in Russian)

Caro G, Kopylova MG, Creaser RA (2004) The hypabyssal 5034 kimberlite of the Gahcho Kue cluster, southeastern slave craton, Northwest Territories, Canada: a granite-contaminated Group-I kimberlite. Can Mineral 42:183–207

Dawson JB (1980) Kimberlites and their xenoliths. Springer, New York, p 252

Drozdov AV, Egorov KN, Gotovcev SP, Klimovsky IV (1989) Hydrogeology and hydrochemical zoning of the Udachnaya kimberlite. In: Complex cryo-hydrogeological investigations. Yakutian Branch of Russian Academy Sciences, Yakutsk, pp 145–146 (in Russian)

Drozdov AV, Iost NA, Lobanov VV (2008) Criohydrogeology of diamond mines of Western Yakutia. Irkutsk State Technical University, Irkutsk, p 508 (in Russian)

Egorov KN, Kornilova VP, Safronov AF, Filippov ND (1986) Micaceous kimberlite from the Udachanaya-East pipe. Trans Russ Acad Sci 291(1):199–202 (in Russian)

Egorov KN, Ushzhapovskaya ZF, Kashaev AA (1988) Zemkorite, the new carbonate from Yakutian kimberlites. Dokl Acad Sci USSR 301(1):188–193 (In Russian)

Field M, Scott Smith BH (1999) Contrasting geology and near-surface emplacement of kimberlite pipes in Southern Africa and Canada. In: Gurney JJ, Gurney JL, Pascoe MD, Richardson SH (eds) 7th International kimberlite conference, vol 1. Red Roof Design, Cape Town, RSA, pp 214–237

Franz GW, Wyllie PJ (1967) Experimental studies in the system CaO-MgO-$SiO_2$-$CO_2$-$H_2O$. In: Wyllie PJ (ed) Ultramafic and related rocks. Wiley, New York, pp 323–326

Golovin AV, Sharygin VV, Pokhilenko NP, Malkovets VG, Kolesov BA, Sobolev NV (2003) Secondary melt inclusions in olivine of unaltered kimberlites of the Udachnaya-East. Trans Russ Acad Sci 388(3):199–202 (in Russian)

Golovin AV, Sharygin VV, Pokhilenko NP (2007) Melt inclusions in olivine from unaltered kimberlites of the Udachnaya-East: some aspects of kimberlite melt evolution on late stages of crystallization. Petrologiya 15(2):178–195 (In Russian)

Ilupin IP, Kaminsky FV, Frantceson EV (1978) Geochemistry of kimberlites. Moskow, Nedra, p 352 (in Russian)

Kamenetsky MB, Sobolev AV, Kamenetsky VS, Maas R, Danyushevsky LV, Thomas R, Pokhilenko NP, Sobolev NV (2004) Kimberlite melts rich in alkali chlorides and carbonates: a potent metasomatic agent in the mantle. Geology 32(10):845–848

Kamenetsky VS, Kamenetsky MB, Sharygin VV, Golovin AV (2007a) Carbonate-chloride enrichment in fresh kimberlites of the Udachnaya-East pipe, Siberia: a clue to physical properties of kimberlite magmas? Geophys Res Lett 34(9):L09316

Kamenetsky VS, Kamenetsky MB, Sharygin VV, Faure K, Golovin AV (2007b) Chloride and carbonate immiscible liquids at the closure of the kimberlite magma evolution (Udachnaya-East kimberlite, Siberia). Chem Geol 237(3–4):384–400

Kamenetsky VS, Kamenetsky MB, Weiss Y, Navon O, Nielsen TFD, Mernagh TP (2009a) How unique is the Udachnaya-East kimberlite? Comparison with kimberlites from the Slave Craton (Canada) and SW Greenland. Lithos 112:334–346

Kamenetsky VS, Maas R, Kamenetsky MB, Paton C, Phillips D, Golovin AV, Gornova MA (2009b) Chlorine from the mantle: magmatic halides in the Udachnaya-East kimberlite, Siberia. Earth Planet Sci Lett 285(1–2):96–104

Khar'kiv AD, Zuenko VV, Zinchuk NN, Kruchkov AI, Ukhanov VA, Bogatykh MM (1991) Kimberlite petrochemistry. TCNIGRI, Yakutsk, p 302 (in Russian)

Khar'kiv AD, Zinchuk NN, Kruchkov AI (1998) Primary diamond deposits of the world. Moscow, NEDRA, p 556 (in Russian)

Klein-BenDavid O, Logvinova AM, Schrauder M, Spetius ZV, Weiss Y, Hauri EH, Kaminsky FV, Sobolev NV, Navon O (2009) High-Mg carbonatitic microinclusions in some Yakutian diamonds—a new type of diamond-forming fluid. Lithos 112S:648–659

Kononov AM (2009) Salty waters and brines of the Olenek aquifer. PhD Thesis, The Institute of the Earth's Crust, Irkutsk, pp 350 (in Russian)

Kopylova MG, Hayman P (2008) Petrology and textural classification of the Jericho kimberlite, Northern Slave Province, Nunavut, Canada. Can J Earth Sci 45:701–723

Kopylova MG, Matveev S, Raudsepp M (2007) Searching for parental kimberlite melt. Geochim Cosmochim Acta 71(14):3616–3629

Kopylova MG, Nowell GM, Pearson DG, Markovic G (2009) Crystallization of megacrysts from protokimberlitic fluids: Geochemical evidence from high-Cr megacrysts in the Jericho kimberlite. Lithos 112 (S1):284–295

Kornilova VP, Egorov KN, Safronov AF, Filippov ND, Zaytsev AI (1998) Mointichellite kimberlite of the Udachnaya pipe and some aspects of the kimberlite melt evolution. Russ Geol 6:48–51 (In Russian)

Kostrovitsky SI (1986) Geochemistry of kimberlite minerals. Novosibirsk, Nauka, p 263 (in Russian)

Kostrovitsky SI, Morikio T, Serov IV, Yakovlev DA, Amirzhanov AA (2007) Isotope and geochemical systematics of the Siberian platform kimberlites. Geol Geophys 48(3):350–371 (in Russian)

Lashkevich VV, Egorov KN (1988) Theoretical modeling of hydrothermal-metasomatic processes in the kimberlites. In: Thermodynamics in geology. Abstracts of the second all-union symposium, vol 1, Miass, pp 139–141 (in Russian)

Maas R, Kamenetsky MB, Sobolev NV, Kamenetsky VS, Sobolev AV (2005) Sr, Nd, and Pb isotope evidence for a mantle origin of alkali chlorides and carbonates in the Udachnaya kimberlite, Siberia. Geology 33(7):549–552

Marshintsev VK, Migalkin KN, Nikolaev NS, Barashkov YuP (1976) Unaltered kimberlite of the Udachnaya-East kimberlite. Dokl Acad Sci USSR, Earth Sci Ser 231(4):961–964 (in Russian)

McDonough WF, Sun SS (1995) The composition of the Earth. Chem Geol 120:223–253

Mernagh TP, Kamenetsky VS, Kamenetsky MB (2012) A Raman microprobe study of melt inclusions in kimberlites from Siberia, Canada, SW Greenland and South Africa. Spectrosc Acta Pt A-Molec Biomolec Spectr 80(1):82–87

Mitchell RH (1986) Kimberlites: mineralogy, geochemistry and petrology. Plenum Press, New York, p 442

Mitchell RH (2006) Petrology of hypabyssal kimberlites. In: Abstract of the kimberlite emplacement workshop, 8th international kimberlite conference, Saskatoon, Sept 2006. http://www.venuewest.com/8IKC/files/00%20zContents.pdf

Novoselov AA (2010) Geochemical modeling of hydrothermal transformation of peridotites of slowly-spreading mid-ocean ridges. PhD Thesis Abstract, Institute of Geochemistry, Russian Academy of Science, Moscow, p 16

Paton C, Hergt JM, Phillips D, Woodhead JD, Shee SR (2007) New insights into the genesis of Indian kimberlites from the Dharwar Craton via in situ Sr isotope analysis of groundmass perovskite. Geology 35(11):1011–1014

Pavlov DI, Ilupin IP (1973) Halite in Yakutian kimberlite, its relations to serpentine and the source of its parent solutions. Dokl Acad Sci USSR, Earth Sci Ser Engl Transl 213:178–180

Polozov AG, Sukhov SS, Gornova MA, Grishina SN (2008a) Salts from Udachnaya-East kimberlite pipe (Yakutia, Russia): occurrences and mineral composition. Extended abstracts of 9IKC-A-00247

Polozov AG, Svensen H, Planke S (2008b) Chlorine isotopes of salts xenoliths from Udachnaya-East kimberlite pipe (Russia). Extended abstracts of 9IKC-A-00249

Scott Smith BH (1996) Kimberlites. Chapter 10, Mineralogical association of Canada short course series. In: Mitchell RH (ed) Undersaturated alkaline rocks: mineralogy, petrogenesis, and economic potential, short course, vol 24, pp 217–243

Seal RR (2006) Sulfur isotope geochemistry of sulfide minerals. In: Sulfide Mineralogy and Geochemistry 61:633–677

Sharp ZD, Barnes JD (2004) Water-soluble chlorides in massive seafloor serpentinites: a source of chloride in subduction zones. Earth Planet Sci Lett 226(1–2):243–254

Sharp ZD, Barnes JD, Brearley AJ, Chaussidon M, Fischer TP, Kamenetsky VS (2007) Chlorine isotope homogeneity of the mantle, crust and carbonaceous chondrites. Nature 446(5):1062–1065

Sharygin VV, Faure K, Golovin AV (2007a) Chloride and carbonate immiscible liquids at the closure of the kimberlite magma evolution (Udachnaya-East kimberlite, Siberia). Chem Geol 237:384–400

Sharygin VV, Kamenetsky VS, Kamenetsky MB, Golovin AB (2007b) Mineralogy and genesis of chloride-bearing nodules from the Udachnaya-East kimberlites. In: Abstracts, international conference on alkaline terrestrial magmatism and its ores. http://geo.web.ru/conf/alkaline/2007/80.pdf, pp 267–271 (in Russian)

Sobolev AV, Sobolev NV, Smith CB, Dubessy J (1989) Fluid and melt compositions in lamproites and kimberlites based on the study of inclusions in olivine. In: Ross J et al (eds) Kimberlites and related rocks: their composition, occurrence, origin and emplacement. Proceedings of the 4th IKC, vol 1. Blackwell Scientific Publications, Sydney, pp 220–241

Sukhov SS (2001) Facies and stratigraphic model of Daldyn-Markha bank: illustration to accumulation mechanism of carbonate deposits on the Siberian craton. In: Lithology and oil-and-gas potential of carbonate deposits. Proceedings of the second all-Russian lithologic conference and 8th all-Russian symposium on fossilized corals and reefs. Syktuvkar, pp 237–239 (in Russian)

Vinogradov VI, Ilupin IP (1972) Isotope compositions of sulfur in kimberlites of the Siberian Platform. Dokl USSR Acad Sci 204(6):1452–1456 (in Russian)

Webster JD (1992) Water solubility and chlorine partitioning in Cl-rich granitic systems—effects of melt composition at 2 kbar and 800 °C. Geoch Cosmoch Acta 56(2):679–687

Woodhead J, Hergt J, Phillips D, Paton C (2009) African kimberlites revisited: in situ Sr-isotope analysis of groundmass perovskite. Lithos 112:311–317

Yoder HS (1986) Potassium-rich rocks—phase-analysis and heteromorphic relations. J Petrol 27(5):1215–1228

Zinchuk NN, Spetsius ZV, Zuenko VV, Zuev VM (1993) The Udachnaya kimberlite pipe. Publishing House of the Novosibirsk University, Novosibirsk, p 147 (in Russian)